Engineering Failure Analysis, Volume 16, Issue 7, October 2009, Pages 2121-2129

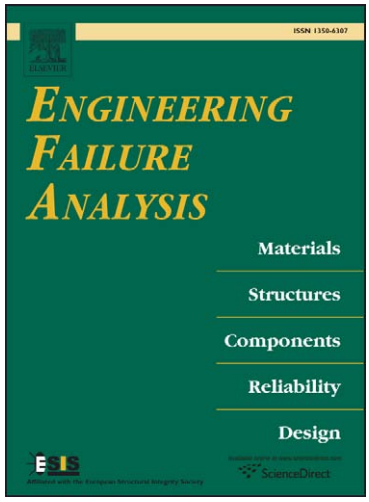

Detecting Natural Crack Initiation and Growth in Slow Speed Shafts with the Acoustic Emission Technology

M. Elforjani, D. Mba

PII: S1350-6307(09)00030-2
DOI: 10.1016/j.engfailanal.2009.02.005
Reference: EFA 1187

To appear in: *Engineering Failure Analysis*

Received Date: 20 November 2008
Revised Date: 26 January 2009
Accepted Date: 2 February 2009

Please cite this article as: Elforjani, M., Mba, D., Detecting Natural Crack Initiation and Growth in Slow Speed Shafts with the Acoustic Emission Technology, *Engineering Failure Analysis* (2009), doi: 10.1016/j.engfailanal.2009.02.005

Detecting Natural Crack Initiation and Growth in Slow Speed Shafts with the Acoustic Emission Technology

M. Elforjani*, D. Mba

School of Engineering, Cranfield University, Cranfield, Beds. MK43 0AL, UK.

*Email: elforjani@gmail.com

Abstract

This paper presents results of an experimental investigation to assess the potential of the Acoustic Emission (AE) technology for detecting natural cracks in operational slow speed shafts. A purpose built test-rig was employed for generating natural degradation on a shaft. It was concluded that AE technology successfully detected natural cracks induced on slow speed shafts.

Keywords: Acoustic Emissions, condition monitoring, natural cracks, shafts.

1 Introduction

Rotating machinery are fatigue loaded machines and operational experience with these machines showed that their components fail high rates which perturbs the normal operating conditions. The primary causes of damages are misalignment, impacting, and cyclic fatigue. Shafts are experience cyclic load conditions, are difficult to access for maintenance and are vulnerable to cracks nucleation and growth. Predicting and preventing the crack phenomenon has attracted the attention of many researchers and has continued to provide a large incentive for the use of condition monitoring techniques to detect the earliest stages of cracks. Slow speed rotating machinery results in reduced energy loss rates from damage related processes and therefore condition monitoring technologies (e.g. vibration analysis) tend to be more difficult to apply. Vibration diagnosis still remains the most widely used method for detecting cracks in rotating machinery though Jamaludin et al [1] summarized the main problems in applying vibration to slow rotating machines. However, the Acoustic Emission (AE) technology is well suited to detecting very small energy release rates. Thus, considerable success has been reported in the application of AE to monitoring slow speed machinery components (e.g. bearings) [1, 2, 3, 4 and 5].

Acoustic Emission (AE) is a term describing a class of phenomenon whereby transient elastic waves are generated by the rapid release of energy from localized sources within or on the surface of a material [6]. Sources of AE in rotating machinery include impacting, friction, turbulence, cavitations, leakage, etc. The typical frequency range associated with AE is between 100 kHz and 1 MHz. Limitations and difficulties in application of AE to machinery has been detailed [7]. Elforjani et al [4 and 5] applied the AE technology to detect natural crack initiation and propagation on slow speed bearings which is one of the few publications that address natural mechanical degradation on rotating machine components. This investigation presents a controlled experiment that ascertains the applicability of the AE technology for monitoring cracks initiation and growth on slow speed shafts.

2 Experimental Program and Setup

The test rig consists of three bearings on one rotating shaft which incorporated a coupling system and an electrical geared motor (MOTOVARIO-Type HA52 B3-B6-B7 j20, 46-Lubricated: AGIP). Two tapered roller bearings, single row (SKF 30207 J2/Q) were employed to support the shaft. An overhang cylindrical roller bearing, single row (SKF NU 1007 ECP) was used to locate the hydraulic load rod onto the shaft. To accelerate crack initiation and growth, a V-Notched shaft of 235 mm length and 35 mm diameter was designed. A radial load was applied to the shaft through the overhang bearing by a hydraulic system (Hi-Force HYDRAULICS-MODEL No: HP110-HAND PUMP-SINGLE SPEED-WORKING PRESSURE: 700 BAR). The design procedures of the shaft are presented in appendix A. The test rig rotational speed was kept constant at 72 RPM. A flexible coupling was employed to absorb any vibration as a result of attaching the shaft to the geared motor, see figure 1. To capture AE's from the rotating shaft a specifically designed oil-bath was constructed onto which an AE sensor was placed, see figure 1. A plastic material was selected for the seals of both oil-bath sides and consequently there was no mechanical contact between the shaft and oil-bath that could result in a noise generation. This enclosed circular bath allowed for direct contact between the rotating shaft and the oil. The enclosed bath was completely filled with oil (CASTROL, Alpha, SP, 460, 3186DM).

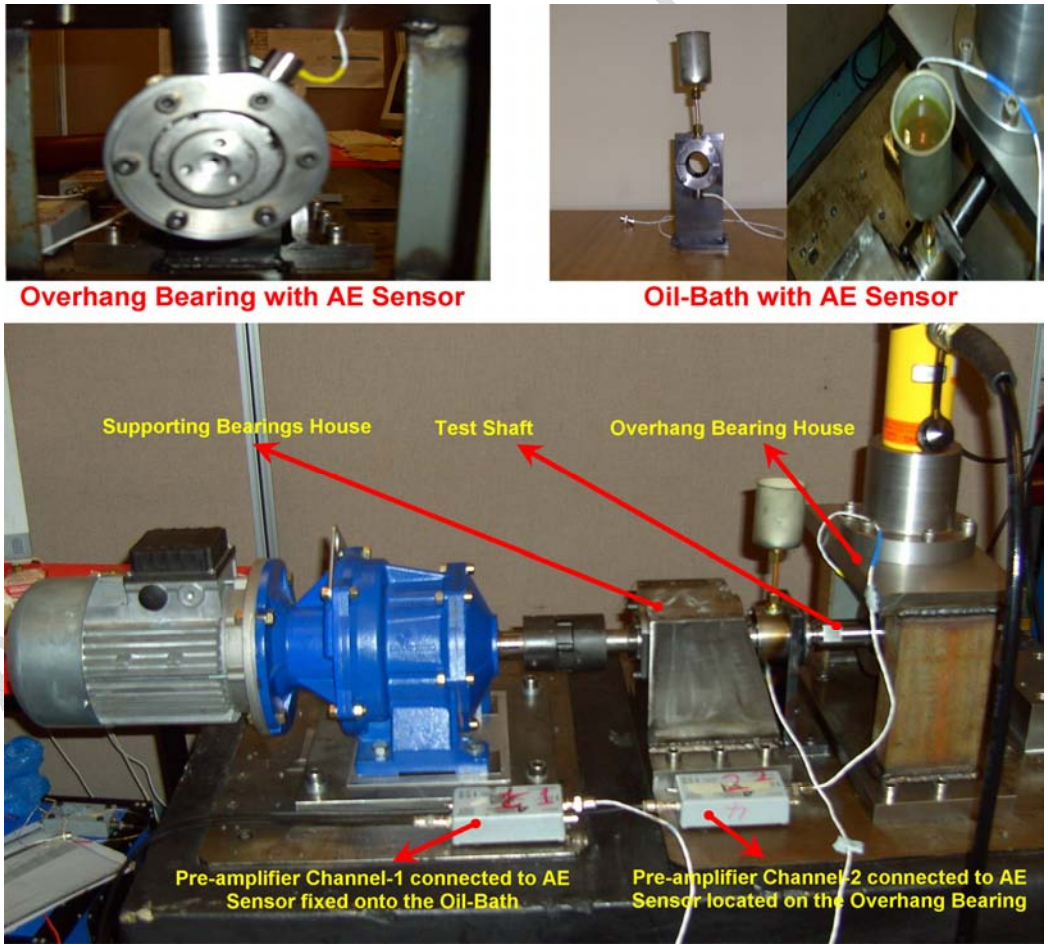

Figure 1 Test rig components.

3 Data Acquisition System

Two Physical Acoustics Corporation WD transducers were employed. These are piezoelectric sensors with a bandwidth of 200-750 kHz. The AE sensors were attached to the overhang bearing and the oil bath using superglue and connected to variable gain preamplifiers 20, 40, and 60dB which were in turn connected to a ruggedized PC, containing Physical Acoustics Corporation PCI-2 acquisition cards. The preamplifiers were set at a gain of 40dB. The software (signal processing package "AEWIN") was incorporated within the PC to monitor AE parameters such as counts, amplitude and absolute energy (recorded at a time constant of 10 ms and sampling rate of 100 Hz). The absolute energy (atto-joules - 10^{-18} joules), is a measure of the true energy and is derived from the integral of the squared voltage signal divided by the reference resistance (10 k-ohms) over the duration of the AE signal. In addition, traditional AE parameters such as counts, amplitude and ASL were also measured. The ASL is a measure of the continuously varying and averaged value of the amplitude of the AE signal in decibels (dB). The ASL is calculated from the r.m.s measurement and is given as:-

$$\mathrm{ASL}\left(\mathrm{dB}\right)=20 \text{ x } \mathrm{Log}_{10}\left(1.4 \text{ x r.m.s in mV}/100\right) \qquad [1]$$

The traditional parameters were calculated over an AE event duration of 1500 μsec and a threshold of 40dB. The threshold value was set at approximately 3dB above operational background noise of the shaft. The system was also continuously set to acquire AE waveforms at a sampling rate of 2 MHz.

4 Results and Discussion

Test shafts were tested until complete fracture prior to which the crack was visually observable. The shaft material properties, the stress range, and the crack size govern the crack propagation rate. One of the key factors that can affect the crack growth rate is the stress at the crack tip. When fracture occurs, the crack will initiate and propagate through the material. It should be noted that the lower stress levels crack initiation and constitutes the majority of the life time before fracture whilst higher stress tends to favour a much short initiation period but a longer crack propagation duration. Under normal conditions of load, shaft material properties, rotational speed and good alignment, it is expected that cracks will be initiated in the vicinity of the notch, where sharp change in cross-sectional area of the shaft was designed, due to the high stress concentration on that site. These cracks will be detected by the AE sensors. For this particular paper two experimental cases are presented that reflect the general observations associated with other experimental tests at loads 4kN and 8kN. Case I is for a load condition of 4kN whilst Case II presents results for a test load of 8kN.

4.1 Case I

The test rig rotational speed was 72 rpm and radial load of 4kN was employed for this particular test. Observations of continuous monitoring of the AE levels, in addition to traditional AE parameters, for 570-mins of shaft operation are presented in figures 2 and 3. The test terminated on fracture of the shaft (570mins). Relatively high levels of AE activity were noted between 95- and 130-mins of operation. After 130-mins

operation the level of AE reduced to that prior to the increased AE activity at 95-mins, see figure 2. It was also observed that at approximately 440-mins into the test AE showed significant increase in AE energy levels until the test was terminated (570-mins). Figure 3 shows trends of traditional AE parameters all of which show significant increase in AE activity from 430-mins of operation. It is also worth noting that relatively high levels of AE parameters (Counts, ASL and Amplitude) at 95-mins of operation were noted, particular the activity associated with AE counts.

Interestingly observations of the AE waveform, sampled at 2MHz showed changing characteristics as a function of time. This is presented in figures 4 and 5 where a typical high transient nature of the waveform of AE events was noted after 100-mins of operation. It is also particularly interesting to note that the AE waveforms after 130-mins of operation did not show any high amplitude transient AE activity. Between 400- to 500-mins of operations high AE transient bursts were again noted until the test was terminated, see figure 5. On termination of the test (570-mins) a visual inspection revealed a fatigue had occurred at the location of V-Notched surface, see figure 10. Also visually observed was the opening and closing of the crack prior to fracture. This movement, which also causes rubbing of the cracked face, results in high AE activity as noted after 456-mins of testing. The authors believe that increased AE activity between 95- to 130-mins is attributed to crack initiation and the large transient AE events towards the end of the tests are due to the rapid propagation, shearing and rubbing of the cracked face.

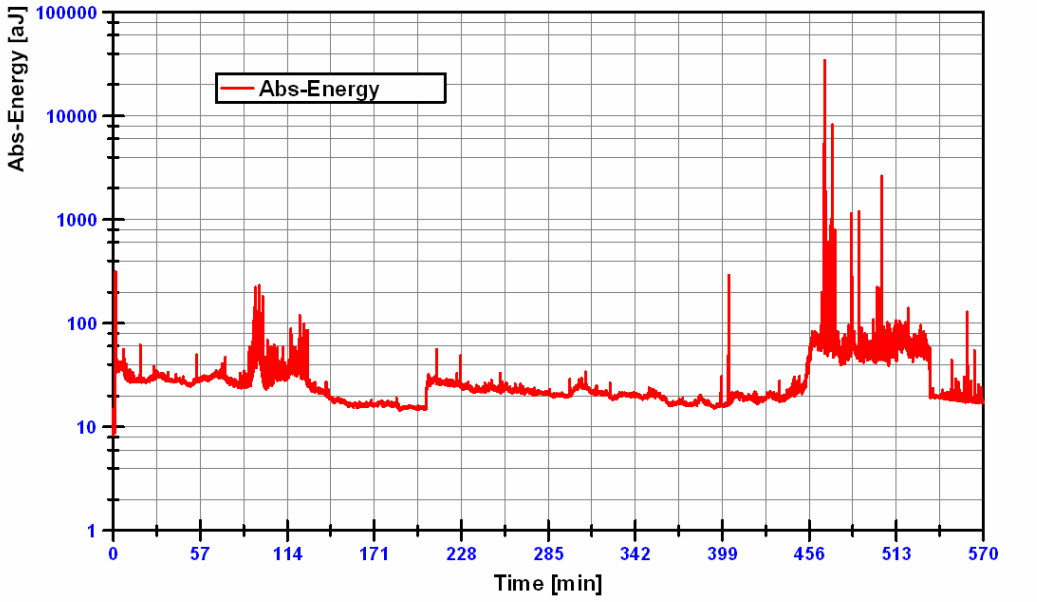

Figure 2 Shaft test results; run to failure.

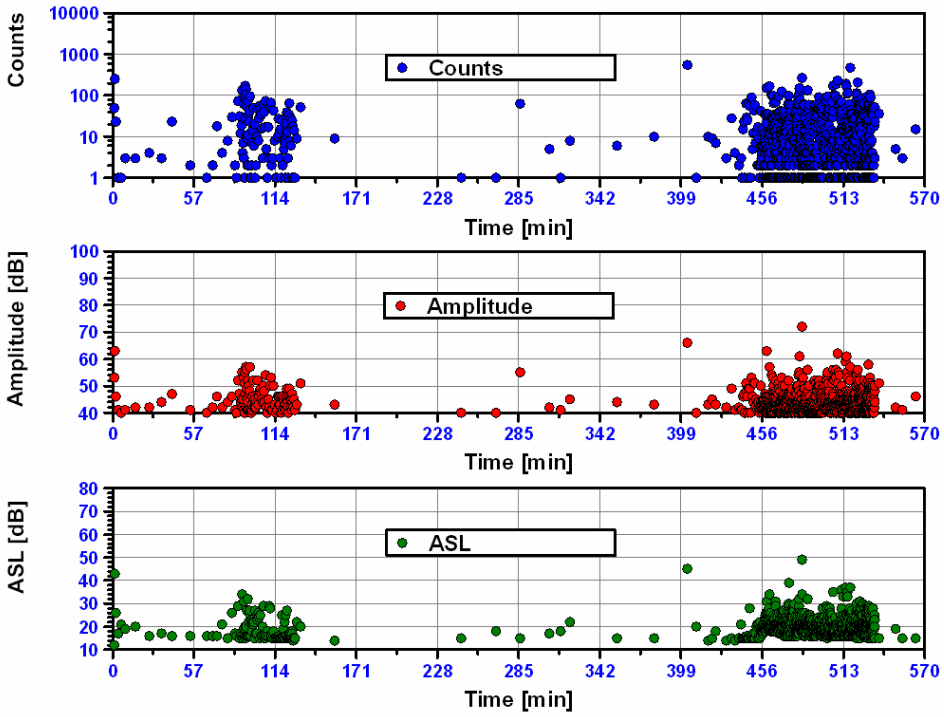

Figure 3 **Classical AE parameters of counts, amplitude and ASL.**

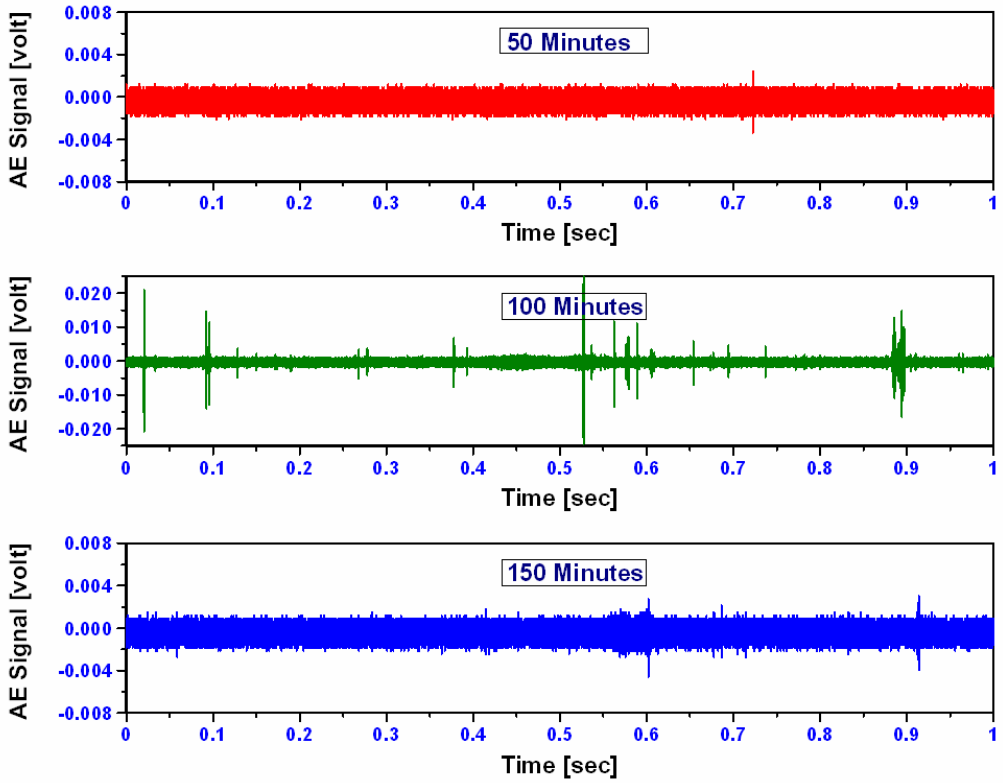

Figure 4 **AE waveforms at 50, 100 and 150 minutes associated with results presented in figure 2.**

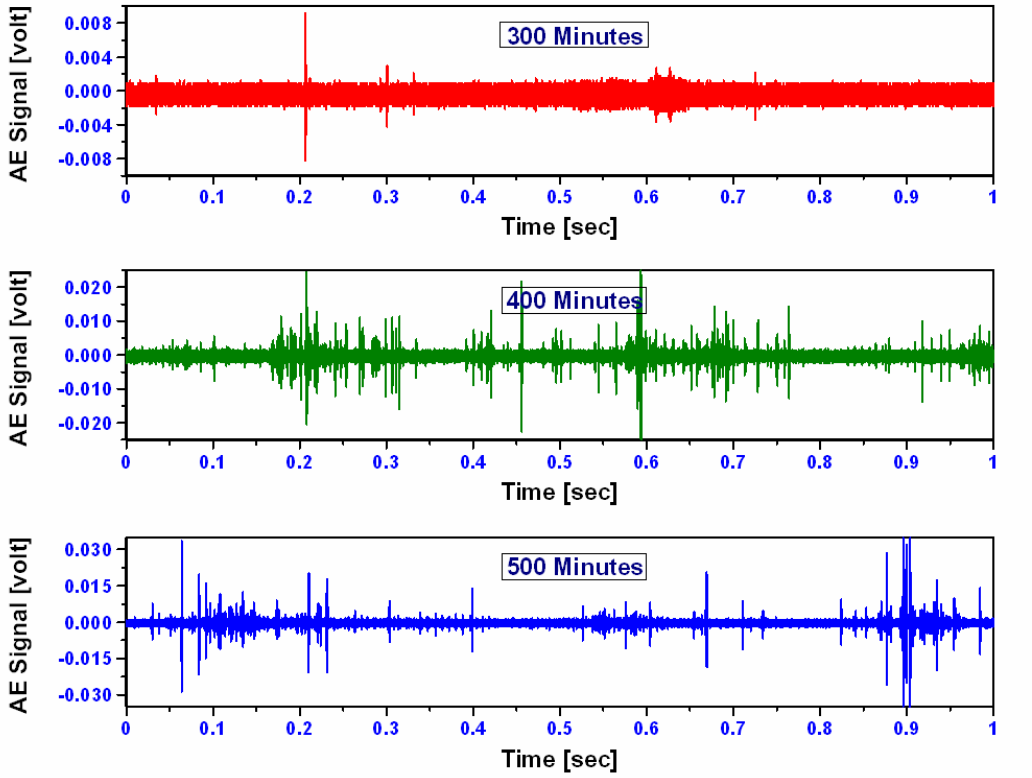

Figure 5 AE waveforms at 300, 400 and 500 minutes associated with results presented in figure 2.

4.2 Case II

The applied load on this test shaft was 8kN. It is worth mentioning that this case presents different trends to that noted in the earlier case. Observations of continuous monitoring of the AE levels, in addition to classical AE parameters, for 130-mins of shaft operation did not show any considerable rise early during testing. During the start of the test steady AE activity was noted. Figure 6 shows the results for the test run until damage was visible; approximately 130-mins of operation. Following the run-in, the measured AE energy remained constant. After approximately 80-mins a large transient rise in AE energy level was observed and this AE activity gradually increased after 90-mins until the test was terminated. The increase in AE energy levels from earlier in the test to the condition of the observable damage was in the order of 34,900%.

As in the previous case the classical AE parameters recorded over the duration of the test is detailed in figure 7, where it was noted that high levels of AE activity were observed at the end of the test; also observed was the opening and closing of the crack. Also noted on the AE waveforms at 100-mins operation was the high transient nature of the waveform. Again clearly showing AE transient events, which grew in amplitude as the test progressed with time, eventually developing very high transient nature of AE events at the end of the test (130-mins), see figures 8 and 9. A very interesting observation of AE waveform (figure 9, 120-mis) shows much larger

duration AE signals which are typically associated with rubbing of mating components. This reinforced the visual observation of the opening and closing of crack as this will cause rubbing of the cracked face. The damage observed for this test conditions is presented in figure 10.

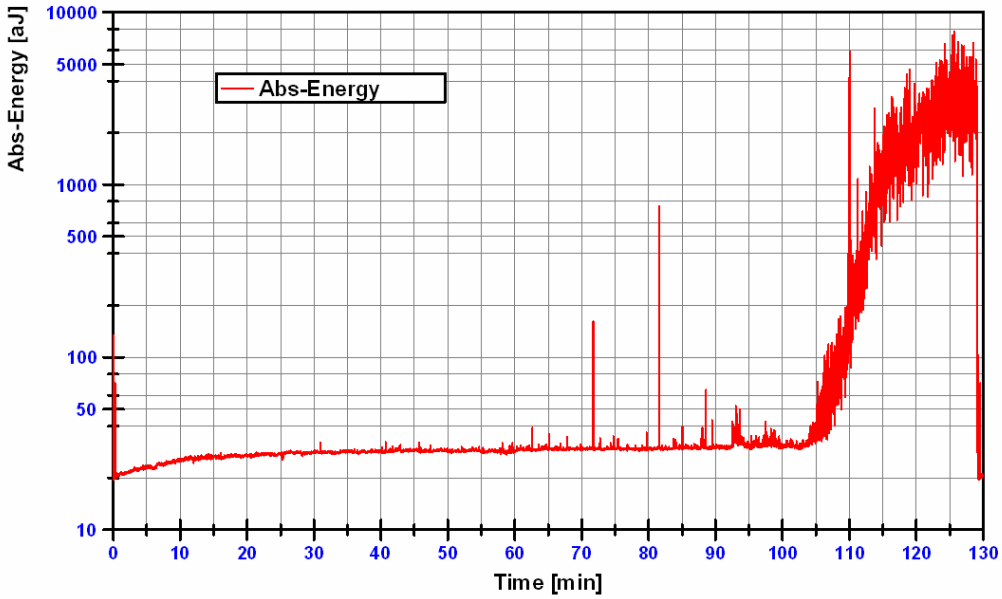

Figure 6 **Shaft test results; run to failure.**

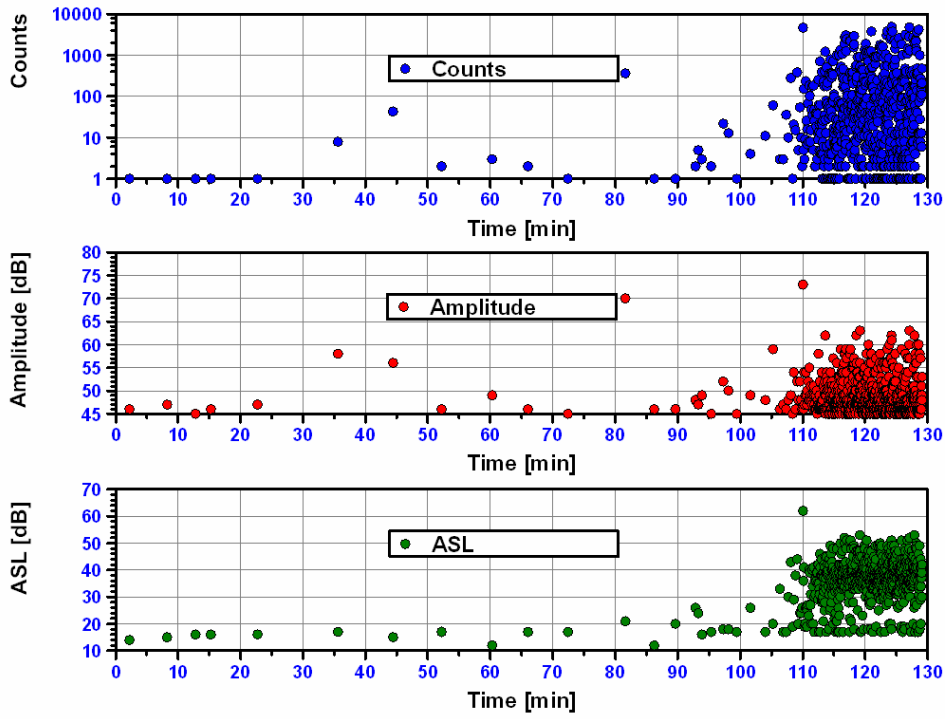

Figure 7 **Classical AE parameters of counts, amplitude and ASL.**

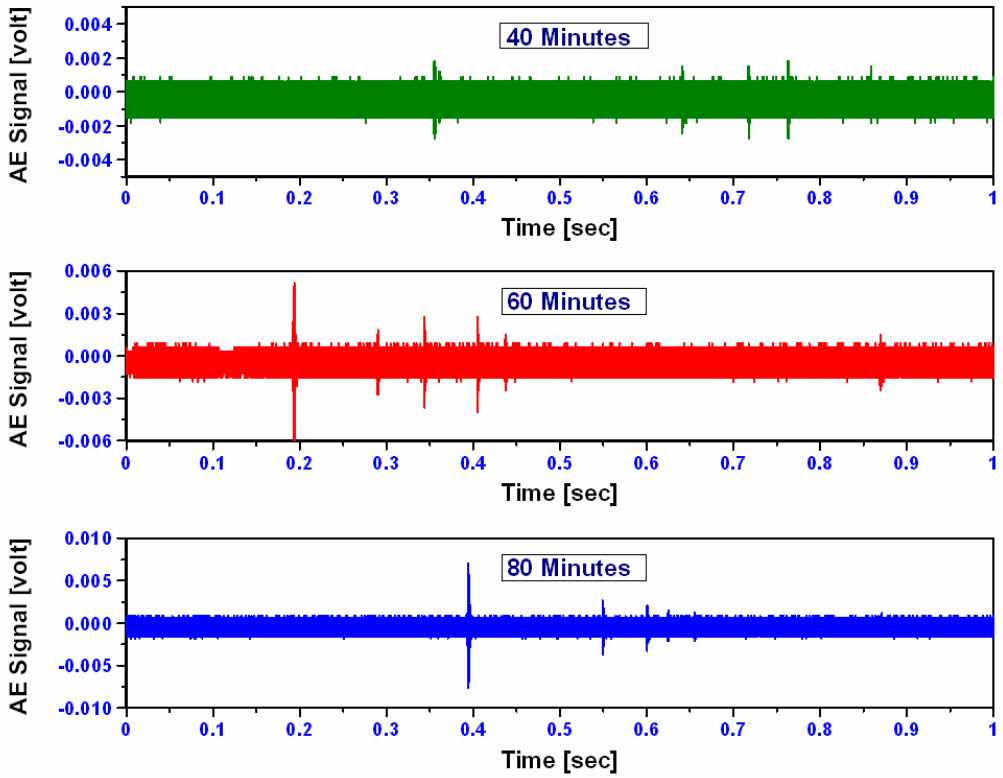

Figure 8 AE waveforms at 40, 60 and 80 minutes associated with results presented in figure 6.

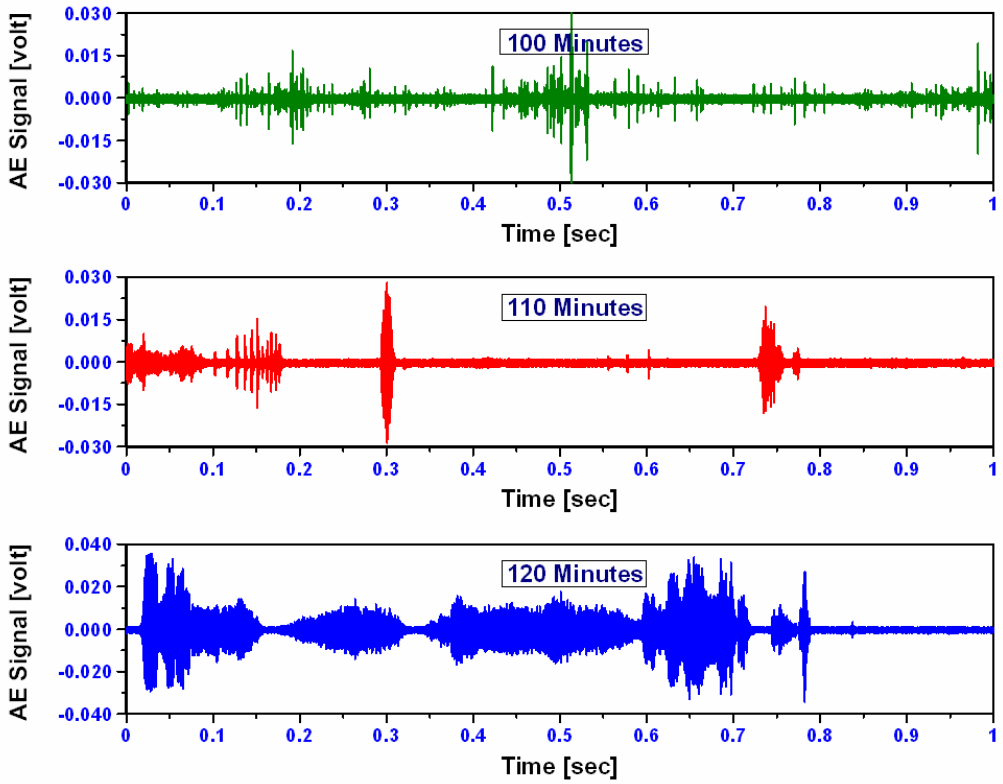

Figure 9 AE waveforms at 100, 110 and 120 minutes associated with results presented in figure 6.

Figure 10 Observed fatigue associated with case I and case II.

The observations of AE for cases I and II show very different characteristics. Firstly, in case I, where the load is half that applied in case II, the relatively early AE activity (95- to 130-mins) was attributed to crack initiation. As the crack propagates immediately after initiation, it is very plausible that AE would have been generated but not at the same intensity and energy levels as noted at the initiation stage. As such the observations of AE between 130-mins to 450-mins were of relatively low level until the crack propagation accelerated to final fracture. In case I, the crack had initiated at V-Notch edges (after 95-mins into testing) eventually leading to a rapid rise in AE until failure of the shaft (456- to 570-mins); the duration between initiation

to the final crack propagation was clearly noted and lasted approximately 320-mins. In case II where relatively higher load was applied there wasn't a clearly defined region where crack initiation can be identified and related to AE activity. This is attributed to the fact that the time between initiation and accelerated crack propagation is much less than at the lower loads, explaining the AE observation noted for case II; the microscopically phase from initiation till the propagation, noted in case I, was not obviously observed due to higher load applied.

5 Conclusion

Shaft run-to-failure tests under natural damage conditions were successfully performed. These tests demonstrated the applicability of AE in detecting crack initiation and propagation on slow speed shafts whilst in operation. The two cases presented are representative of other tests performed in this study. It is concluded that there is a clear correlation between increasing AE energy levels and the natural propagation and formation of shaft defects. The study has also demonstrated that AE parameters such as counts, amplitude and ASL are reliable, robust and sensitive to the detection of natural incipient cracks and surface damages in slow speed shaft. This work is the first known attempt at correlating AE activity and natural defect generation in slow speed rotating shafts and it is also the first known attempt at monitoring the mechanical integrity of rotating shafts.

6 References

1 Jamaludin, N.; Mba, D.; Bannister, R., H., Condition Monitoring of Slow-Speed Rolling Element Bearings Using Stress Waves, Proceedings of the IMECHE Part E Journal of Process Mechanical Engineering, Volume 215, Number 4, 1 November 2001, pp. 245-271(27), Publisher: Professional Engineering Publishing.

2 Mba, D.; Rao, Raj, B., K., N., Development of Acoustic Emission Technology for Condition Monitoring and Diagnosis of Rotating Machines: Bearings, Pumps, Gearboxes, Engines, and Rotating Structures. The Shock and Vibration Digest 2006 38: 3-16.

3 Miettinen, J.; Pataniitty, P., Acoustic Emission in Monitoring Extremely Slowly Rotating Rolling Bearing, Proceedings of 12th International Congress on Condition Monitoring and Diagnostic Engineering Management, COMADEM 99, England.

4 M. Elforjani, D. Mba, Natural mechanical degradation measurements in slow speed bearings, Engineering Failure Analysis, Volume 16, Issue 1, January 2009, Pages 521-532.

5 M., Elforjani; D., Mba, Monitoring the Onset and Propagation of Natural Degradation Process in a Slow Speed Rolling Element Bearing With Acoustic Emission, Journal of Vibration and Acoustics, volume 130, Issue 4, 041013 (Published Online, 15 July 2008).

6 FDIS ISO 22096; Condition monitoring and diagnosis of machines – Acoustic Emission 2007.

7 J.Z. Sikorska and D. Mba, Truth, Lies Acoustic Emission and Process Machines, Journal of Mechanical Process Engineering, Part E, IMechE, Volume 222, Number 1, 1-19, 2008.

8 Joseph, Edward, Shigley; Charles, R., Mischke, Mechanical Engineering Design, Fifth Edition (International Edition), Mechanical Engineering Series, 1989, McGraw-Hill Book Co., Singapore.

9 Peter, R., N., Childs, Mechanical Design, 1998, Antony Rowe Ltd, Eastbourne, UK.

10 Walter, D., Pilkey, Peterson's Stress Concentration Factors, Second Edition, 1997, John Wiley & Sons, Inc., New York, United States of America.

7 Appendix A

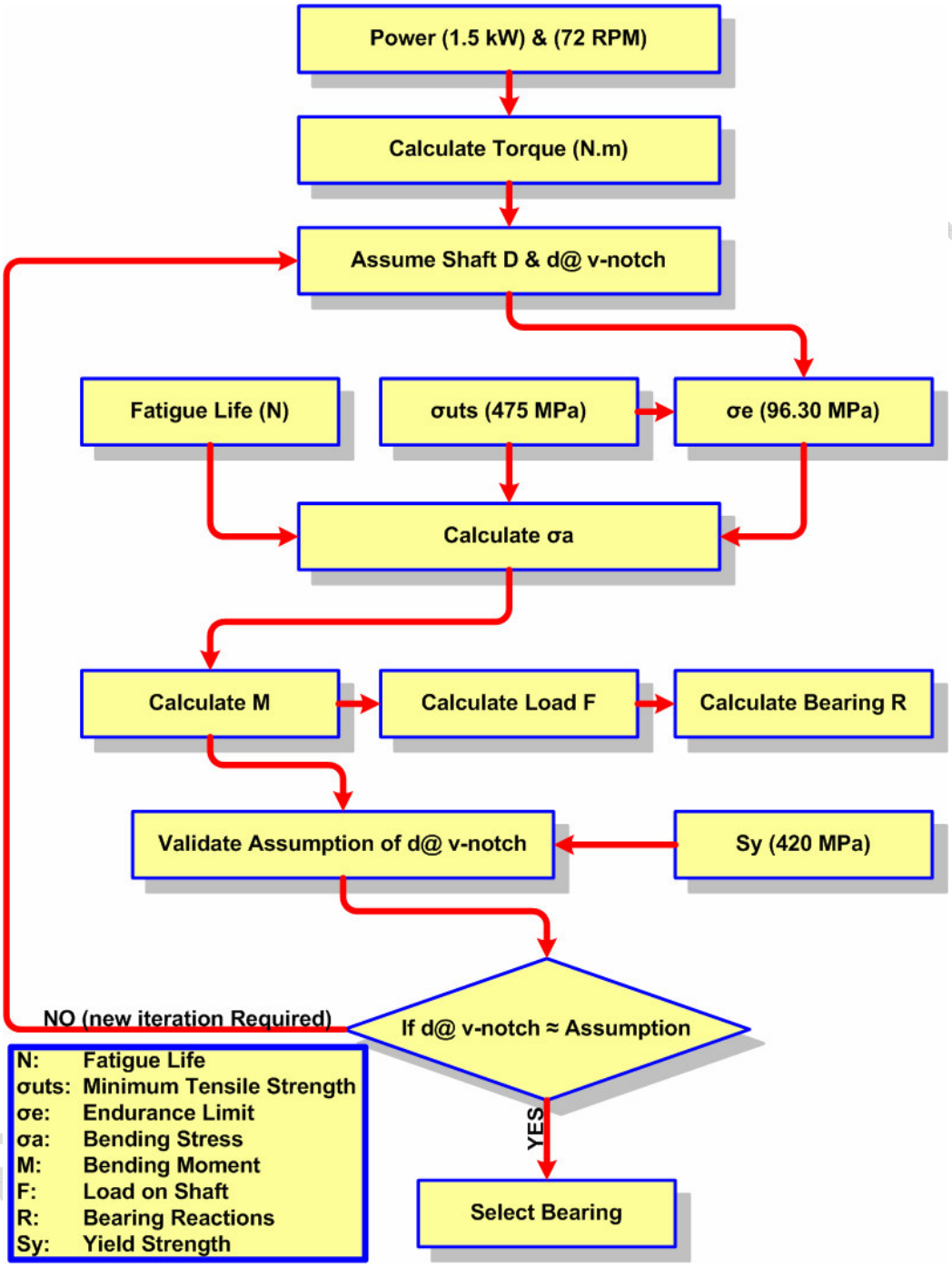

Figure A1 Shaft design flow chart

Equations and Factors used in the Shaft Design [8, 9 and 10]

Shaft material Type: **Low Carbon Steel.**

Minimum Tensile Strength (σuts) = 475 MPa.

Yield Strength (Sy) = 420×10^6 N/m^2.

Fatigue Life (N) = 36,000 cycles at 4kN.

Fatigue Life (N) = 10,800 cycles at 8kN.

Safety Factor (n) =2.

$$\text{Torque (T)} = \frac{9550\ P}{RPM} \quad (1.1)$$

$$\text{Bending Stress } (\sigma_a) = a\ N^b \quad (1.2)$$

$$\text{Endurance Limit } (\sigma_e) = k_a k_b k_c k_d k_e k_f k_g \sigma'_e \quad (1.3)$$

The surface finish factor (k_a) = 0.88, the size factor (k_b) = 0.874, the load factor (k_c) =1, the temperature factor (k_d) =1, the duty cycle factor (k_e) =1, the fatigue stress concentration factor (k_f) = 0.523, the miscellaneous factors (k_g) = 1, and the endurance limit of test specimen (σ'_e) = 239.4MPa.

$$a = \frac{(0.9\sigma_{uts})^2}{\sigma_e} \quad (1.4)$$

$$b = -\frac{1}{3}\log\left(\frac{0.9\sigma_{uts}}{\sigma_e}\right) \quad (1.5)$$

$$\text{Bending Stress at V-Notch } (\sigma_{normal@\ Notch}) = \frac{32M_{@Notch}}{\pi d^3} \quad (1.6)$$

$$\text{Sheer Stress at V-Notch } (\tau_{normal}) = \frac{16T}{\pi d^3} \quad (1.7)$$

$$\text{Load (F)} = \frac{2M_{@Notch}}{a} \quad (1.8)$$

$$\text{Maximum Bending Stress } (\sigma_{normal@\ x}) = \frac{32M_{max}}{\pi D^3} \quad (1.9)$$

$$\text{Shaft Diameter at V-Notch } (d^3_{@Notch}) = \frac{32n}{\pi S_y}\sqrt{M^2_{@Notch} + T^2} \quad (1.10)$$

Shaft Diameter (D) = 35mm.
Shaft Diameter at V-Notch (d) = 25mm.